Modulation structure in $Bi_2(La_{1-x}Ca_{1+x})CuO_{6.5+\delta}$ and $(Bi_{2-x}Pb_x)LaCaCuO_{6.5+\delta}$ systems

Mao Zhiqiang, Tian Mingliang, Tan Shun, Zuo Jian, Xu Yang, Wang Yu, and Xu Chunyi
Structure Research Laboratory, University of Science and Technology of China, Hefei, Anhui 230026, People's Republic of China

Zhang Yuheng
Structure Research Laboratory, University of Science and Technology of China, Hefei, Anhui 230026, People's Republic of China and Chinese Center of Advanced Science and Technology (World Laboratory), Beijing 100080, People's Republic of China

(Received 5 May 1993; revised manuscript received 26 October 1993)

The microstructure of Sr-free bismuth cuprates, i.e., $Bi_2(La_{1-x}Ca_{1+x})CuO_{6.5+\delta}$ and $(Bi_{2-x}Pb_x)LaCaCuO_{6.5+\delta}$, was determined by means of x-ray diffraction and electron diffraction (ED). ED analysis revealed that the two types of Sr-free compounds possess a monoclinic superstructural modulation, which is similar to $Bi_2Sr_2CuO_{6+\delta}$. In the $Bi_2(La_{1-x}Ca_{1+x})CuO_{6.5+\delta}$ system, the modulation wavelength along the *b* and *c* axes increased markedly with the Ca substitution for La. At the same time this substitution facilitated the commensurate-to-incommensurate transition. For the $(Bi_{2-x}Pb_x)LaCaCuO_{6.5+\delta}$ system, a similar change in the modulation wave vector was also observed. The dependence of the modulation vector on chemical composition can be best interpreted by the crystal-misfit model. In addition, Raman scattering analysis of the $Bi_2(La_{1-x}Ca_{1+x})CuO_{6.5+\delta}$ system showed that the vibrational properties of the oxygen atoms in the Bi-O bonding also changed with the increase in the modulation wavelength, and this behavior can be regarded as a consequence of the structural relaxation caused by the enhancement of the degree of crystal fit.

I. INTRODUCTION

As is well known, the superconductivity of the bismuth cuprates, $Bi_2Sr_2Ca_{n-1}Cu_nO_{2n+4+\delta}$ $(n=1,2,3)$, originates from the copper-oxygen layer. But the influence of normal layers, i.e., of the strontium- and bismuth-oxygen layers, on the superconducting properties is still subject of controversy. A study of the replacement of strontium by other elements in these oxides is necessary in order to understand the relationship between structure, chemical bonding, and superconductivity. Takemura *et al.* [1] and Inoue *et al.*[2] successfully synthesized a new family of Sr-free Bi-based compounds, i.e., $Bi_2LaCaCuO_{6.5+\delta}$ and $Bi_2La_xCa_{3-x}Cu_2O_{8.5+\delta}$. The two Sr-free compounds are isostructural to the Bi 2:2:0:1 and Bi 2:2:1:2 phases respectively. Superconductivity near 50 K was reported in $Bi_2La_xCa_{3-x}Cu_2O_{8.5+\delta}$ with $x=0.5$, but semiconductivity in $Bi_2LaCaCuO_{6.5+\delta}$. Obviously, systematic investigation of the crystal microstructure as well as the superconducting properties of the Sr-free Bi-based compounds is of great importance to clarify the role the SrO layer plays in the occurrence of superconductivity in the Bi cuprates.

In this paper, we report on the microstructural characteristics of $Bi_2LaCaCuO_{6.5+\delta}$ and its substituted systems, i.e., $Bi_2(La_{1-x}Ca_{1+x})CuO_{6.5+\delta}$ $(0.2\le x\le 0.8)$ and $(Bi_{2-x}Pb_x)LaCaCuO_{6.5+\delta}$ $(0.1\le x\le 0.5)$.

II. EXPERIMENTAL METHODS

Samples with nominal compositions of $Bi_2(La_{1-x}Ca_{1-x})CuO_{6.5+\delta}$ $(x=0,0.2,0.6,0.8)$ and $(Bi_{2-x}Pb_x)LaCaCuO_{6.5+\delta}$ $(x=0.1,0.3,0.5)$ were prepared by regular solid-state reaction using high-purity powders of Bi_2O_3, La_2O_3, $CaCO_3$, PbO and CuO. First, the appropriate mixture of these powders was well ground and calcined at about 850 °C for 20 h in air. The calcined samples were thoroughly reground and pressed into disk-shaped pellets. The pellets were sintered in the temperature range of 880–900 °C and finally quenched in air.

X-ray-diffraction (XRD) analysis was carried out with a Rigaku-D/max-γA diffractometer using monochromatic high-intensity Cu- Kα radiation at room temperature. Electron-diffraction (ED) patterns were obtained using an H-800 transmission electron microscope (TEM), and the specimens for TEM observations were prepared by the ion-milling method. Raman spectra were measured on a Spex-1403 Raman spectrophotometer using a back-scattering technique. The 5145-Å line from an argon-ion laser was used as an excitation light source. All measurements were made at room temperature, and each spectrum shown was taken with refocusing on at least two different spots to assure reproducibility.

III. EXPERIMENTAL RESULTS

A. XRD analyses for the samples $Bi_2(La_{1-x}Ca_{1+x})CuO_{6.5+\delta}$ $(0\le x\le 0.8)$ and $(Bi_{2-x}Pb_x)LaCaCuO_{6.5+\delta}$ $(0.1\le x\le 0.5)$

Figures 1(a) and 1(b) show the composition change of the XRD pattern for $Bi_2(La_{1-x}Ca_{1+x})CuO_{6.5+\delta}$ and $(Bi_{2-x}Pb_x)LaCaCuO_{6.5+\delta}$. From the two figures, it can be seen that the traces of the main phase [marked with dots in Figs. 1(a) and 1(b)] of these Sr-free compounds are similar to that of $Bi_2Sr_2CuO_{6+\delta}$. The ideal single-phase

TABLE I. Structural parameters of the samples $Bi_2(La_{1-x}Ca_{1+x})CuO_{6.5+\delta}$ and $(Bi_{2-x}Pb_x)LaCaCuO_{6.5+\delta}$. *M*: the type of modulation, *I*: incommensurate, *C*: commensurate. (The error in the lattice constants is about 2/1000.)

	$Bi_2(La_{1-x}Ca_{1+x})CuO_{6.5+\delta}$				$(Bi_{2-x}Pb_x)LaCaCuO_{6.5+\delta}$		
x	0.8	0.6	0.2	0	0.1	0.3	0.5
a (Å)	5.382	5.383	5.386	5.381	5.424	5.425	5.420
b (Å)	5.302	5.354	5.386	5.391	5.424	5.409	5.398
c (Å)	23.832	23.820	23.739	23.711	23.801	23.813	23.799
M	*I*	*I*	*C*	*C*	*C*	*C*	*I*

samples are only obtained in the samples with the nominal compositions of $Bi_2LaCaCuO_{6.5+\delta}$, $Ba_2La_{0.8}Ca_{1.2}CuO_{6.4+\delta}$, and $Bi_{1.9}Pb_{0.1}LaCaCuO_{6.4+\delta}$; whereas some impurity phases [marked with arrows in Figs. 1(a) and 1(b)] are present in other samples. Comparison of these data with data from the parent compound, $Bi_2Sr_2CuO_{6+\delta}$, shows that the phases of these Sr-free compounds are isostructural to $Bi_2Sr_2CuO_{6+\delta}$. The unit-cell parameters of each sample obtained from least-squares refinement are displayed in Table I. For the $Bi_2(La_{1-x}Ca_{1+x})CuO_{6.5+\delta}$ system, Ca^{2+} replacement for La^{3+} intensifies the orthorhombicity of the Sr-free 2:2:0:1 phase. The length of the *b*-axis decreases strikingly with increase in the ratio of Ca to La, while the *a* axis almost remains intact. It is of interest to note that this type of substitution induces an increase in the length of the *c* axis. However, for the $(Bi_{2-x}Pb_x)LaCaCuO_{6.5+\delta}$ system, the partial substitution of Pb for Bi has no apparent influence on the length of the *a* and *c* axes, while the *b* axis exhibits a very slight decrease with increase in Pb content.

B. ED analyses for the samples $Bi_2(La_{1-x}Ca_{1+x})CuO_{6.5+\delta}$ $(0 \le x \le 0.8)$ and $(Bi_{2-x}Pb_x)LaCaCuO_{6.5+\delta}$ $(0.1 \le x \le 0.5)$

Figures 2(a)–2(d) show the [100]-zone-axis ED patterns of the samples $Bi_2(La_{1-x}Ca_{1+x})CuO_{6.5+\delta}$ with $x = 0$, 0.2, 0.6, and 0.8. From these ED patterns, it is clear that satellite reflections appear in each sample. This implies that superstructural modulation also exists in the Sr-free Bi cuprates, and its supercell, similar to that of $Bi_2Sr_2CuO_{6+\delta}$, is monoclinic. From the four [100] ED patterns, the corresponding modulation vectors in the b^*-c^* plane, $q^* = \beta b^* + \gamma c^*$ can be identified as

$$q_1^* = 0.25b^* + 0.93c^* \quad (x = 0),$$

$$q_2^* = 0.25b^* + 0.86c^* \quad (x = 0.2),$$

$$q_3^* = 0.23b^* + 0.60c^* \quad (x = 0.6),$$

$$q_4^* = 0.22b^* + 0.54c^* \quad (x = 0.8),$$

respectively. [The estimated error for the modulation vector, $\Delta\beta$ (or $\Delta\gamma$) ≤ 0.005.] It is apparent that both the b^* and c^* components of the modulation vector decrease with an increase of the ratio of Ca to La, and the variation of the c^* component is much more striking than that of the b^* component. This suggests that the wavelength of the superstructural modulation along the *b* and *c* axes increases with the substitution of Ca for La. On the other hand, we also find that the modulation in the samples with $x = 0, 0.2$ is commensurate along the *b* axis but is incommensurate in the samples with $x = 0.6, 0.8$. That is to say, Ca substitution for La simultaneously facilitates the commensurate-to-incommensurate transition.

Figures 3(a)–3(c) show the [100]-zone-axis ED patterns of the samples $(Bi_{2-x}Pb_x)LaCaCuO_{6.5+\delta}$ with $x = 0.1$, 0.3, and 0.5. The corresponding modulation wave vectors obtained from these ED patterns can be expressed as follows:

$$q_1^* = 0.25b^* + 0.83c^* \quad (x = 0.1),$$

$$q_2^* = 0.25b^* + 0.79c^* \quad (x = 0.3),$$

$$q_3^* = 0.24b^* + 0.75c^* \quad (x = 0.5),$$

Clearly, in the $(Bi_{2-x}Pb_x)LaCaCuO_{6.5+\delta}$ system, Pb replacement of Bi has less influence on the modulation vector. The values of β and γ exhibit only a slight reduction with increase of the Pb content. Nevertheless, this substitution also causes a transition from commensurability to incommensurability in the superstructural modulation.

Here, it should also be mentioned that Pb substitution for Bi in the $(Bi_{2-x}Pb_x)LaCaCuO_{6.5+\delta}$ system differs from that in $Bi_{2-x}Pb_xSr_2CuO_{6+\delta}$. In $Bi_{2-x}Pb_xSr_xCuO_{6+\delta}$, Pb intercalation in the Bi_2O_2 layers induces a kind of orthorhombic Pb-type modulation,[3] which, however, is not observed in the $(Bi_{2-x}Pb_x)LaCaCuO_{6.5+\delta}$ system.

C. Raman-scattering analyses for the samples $Bi_2(La_{1-x}Ca_{1+x})CuO_{6.5+\delta}$ $(0 \le x \le 0.8)$

Figure 4 shows the Raman spectra of the samples $Bi_2(La_{1-x}Ca_{1+x})CuO_{6.5+\delta}$ with $x = 0$, 0.2, 0.6, and 0.8 in the frequency range 170–800 cm^{-1}. First, for the $x = 0$ sample, two strong Raman modes at 456 and 630 cm^{-1} are clearly observed. Second, for the case of $x > 0$, the variation of the Raman spectra caused by Ca substitution fo La can be described as follows: (i) the position of the higher-frequency mode shifts from 630 cm^{-1} for $x = 0$ to 645 cm^{-1} for $x = 0.8$, while its relative intensity and linewidth decrease markedly with increase in the ratio of Ca to La, (ii) the position and intensity of the Raman mode at the lower-frequency side ($\sim$456 cm^{-1}) hardly varies with change in the ratio of Ca to La. Overall, the Raman modes observed in $Bi_2(La_{1-x}Ca_{1+x})CuO_{6.5+\delta}$ are very similar to those of polycrystalline $Bi_2Sr_2CuO_{6+\delta}$ in the same frequency range. Therefore, based on Raman-

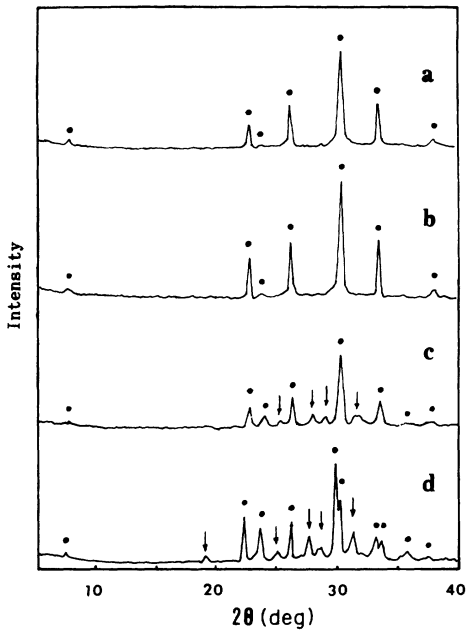

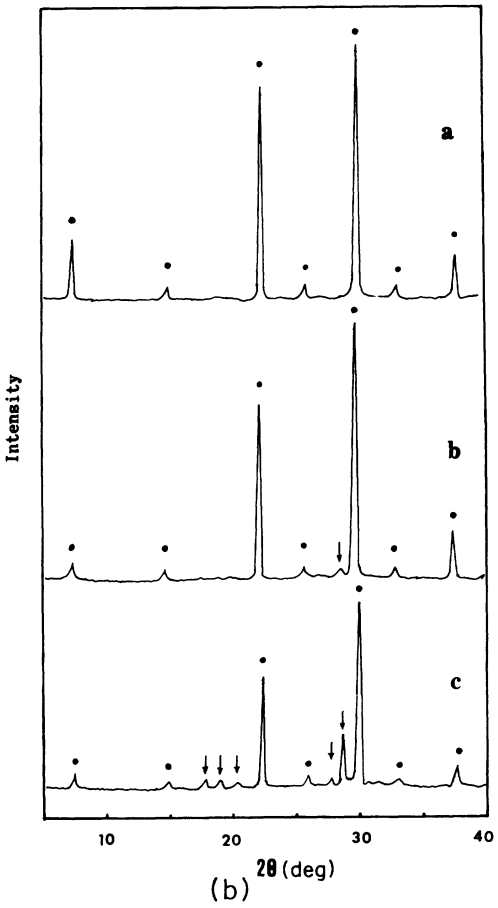

FIG. 1. (a) XRD patterns of the samples $Bi_2(La_{1-x}Ca_{1+x})CuO_{6.5+\delta}$; a, $x=0$; b, $x=0.2$; c, $x=0.6$; d, $x=0.8$. (b) XRD patterns of the samples $(Bi_{2-x}Pb_x)LaCaCuO_{6.5+\delta}$; a, $x=0.1$; b, $x=0.3$; c, $x=0.5$. The peaks marked with dots correspond to the reflections of the Sr-free Bi 2:2:0:1 phase, while those marked with arrows correspond to the reflections of the impurity phases.

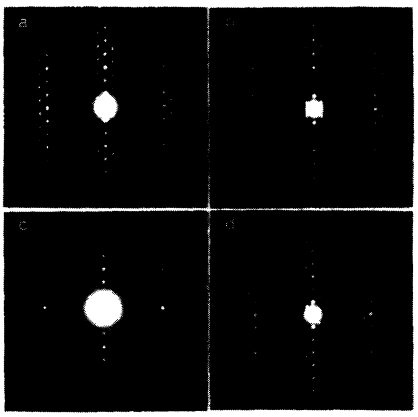

FIG. 2. [100]-zone-axis ED patterns of the samples $Bi_2(La_{1-x}Ca_{1+x})CuO_{6.5+\delta}$; a, $x=0$; b, $x=0.2$; c, $x=0.6$; d, $x=0.8$.

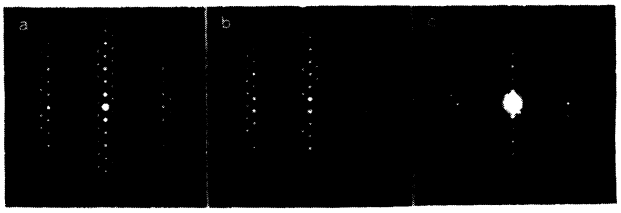

FIG. 3. [100]-zone-axis ED patterns of the samples $(Bi_{2-x}Pb_x)LaCaCuO_{6.5+\delta}$; a, $x=0.1$; b, $x=0.3$; c, $x=0.5$.

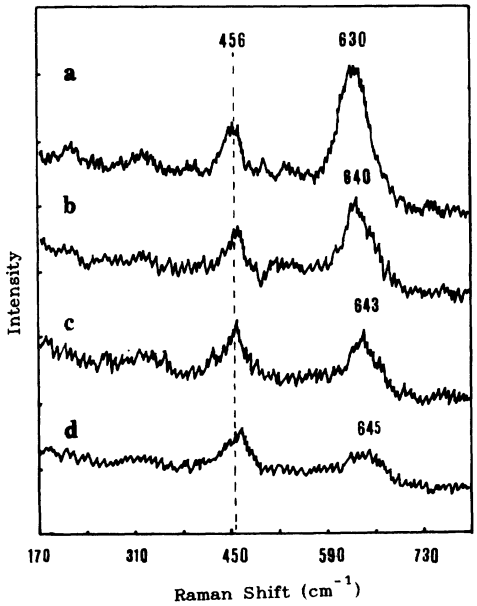

FIG. 4. Raman spectra of the samples $Bi_2(La_{1-x}Ca_{1+x})CuO_{6.5+\delta}$; a, $x=0$; b, $x=0.2$; c, $x=0.6$; d, $x=0.8$.

scattering analyses of $Bi_2Sr_2CuO_{6+\delta}$,[4-6] the Raman mode characteristic of $Bi_2(La_{1-x}Ca_{1+x})CuO_{6.5+\delta}$ can be assigned. For the $Bi_2Sr_2CuO_{6+\delta}$ system, it is now well established that the $\sim$450-cm^{-1} and $\sim$630-cm^{-1} modes correspond to the vibrations of O_{Sr} and O_{Bi} atoms, respectively (O_{Sr} and O_{Bi} refer to oxygen atoms residing in the SrO and BiO layers). So, for the $Bi_2(La_{1-x}Ca_{1+x})CuO_{6.5+\delta}$ system, the Raman mode at about 630–645 cm^{-1} can also be considered to originate from the vibration of the O_{Bi} atom, while the $\sim$456-cm^{-1} mode possibly comes from O_{Ca} and O_{La} vibration. This postulation is consistent with the assumption proposed by Takemura *et al.*[1] that in the $Bi_2LaCaCuO_{6.5+\delta}$ system the (La,Ca) atoms are likely to occupy the Sr sites in the perovskite block.

In addition, another noteworthy point for the Raman spectra shown in Fig. 4 is that the lineshape of the Raman peak with the frequency of 630, 640, 643, and 645 cm^{-1} is asymmetric; a weaker broadening around $\sim$660–670 cm^{-1} is observed for each sample. However, in the $Bi_2Sr_2CuO_{6+\delta}$ system, a weak shoulder peak around 660 cm^{-1} always appears at the higher-frequency side of the 630-cm^{-1} mode.[4-5] Cardona and co-workers[4] ascribed the presence of such a shoulder peak to the vibration of the extra oxygen atoms of the Bi_2O_2 layers. For samples of $Bi_2(La_{1-x}Ca_{1+x})CuO_{6.5+\delta}$, though no obvious shoulder peak around 660–670 cm^{-1} is detected, the broadening of the Ramon mode (630–645 cm^{-1}) in this frequency range can similarly be considered to come from the vibration of the extra oxygen atoms of the Bi_2O_2 layers. Finally, it should be pointed out that we did not analyze the Raman spectra of $(Bi_{2-x}Pb_x)LaCaCuO_{6.5+\delta}$ owing to the fluorescence of the impurity phases.

IV. DISCUSSION

A. The origin of superstructural modulation in the Sr-free Bi cuprates

It has been realized that in Bi cuprates the double BiO layers do not consist of perfect two-dimensional sheets, but contain an alternating distribution of Bi-concentrated bands and Bi-deficient bands. This type of arrangement of Bi atoms forms the superstructural modulation. As to its origin, several models have been proposed in previous work,[7-9] including: (1) the extra-oxygen model, (2) ordering of Sr vacancies, (3) regular substitution of Bi by (Ca,Sr) or Cu, and (4) changes in the orientation of Bi lone pairs. The extra-oxygen model indicates that the periodic intercalation of extra oxygen atoms in the Bi_2O_2 layers is responsible for the superstructural modulation. But recently some authors[10] suggested that the oxygen excess in the Bi_2O_2 layers cannot be regarded as the origin of modulation but is a consequence of a particular geometry introduced by bismuth. Hence, the origin of the modulation requires further clarification.

In our earlier work,[11] when we compared the modulation structure of $Bi_{2.1}Sr_{1.9-x}La_xCuO_{6+\delta}$, $Bi_2Sr_{2-x}Ba_xCuO_{6+\delta}$, and $Bi_{2-x}Pb_xSr_2CuO_{6+\delta}$, we found that the crystal-misfit model is much more effective in interpreting the modulation-vector change induced by doping with different elements. This model indicates that the superstructural modulation of Bi cuprates comes from the crystal misfit along the b axis between the Bi_2O_3 of the BiO layer and the perovskite blocks. The degree of crystal misfit mainly depends on the size of the perovskite block (primarily the length of the b axis); the larger the b parameter, the lower the degree of crystal fit. The crystal-misfit model can also give a better interpretation for the variation of the modulation wave vector observed in the $Bi_2(La_{1-x}Ca_{1+x})CuO_{6.5+\delta}$ and $(Bi_{2-x}Pb_x)LaCaCuO_{6.5+\delta}$ systems. XRD analysis has shown that for the $Bi_2(La_{1-x}Ca_{1+x})CuO_{6.5+\delta}$ system the b axis exhibits an apparent decrease with increase in the ratio of Ca to La. For this reason, the degree of crystal fit between the(La,Ca)-Cu-O perovskite blocks and the BiO rocksalt units is enhanced, thus resulting in relaxation of the distorted BiO layer. Therefore the modulation wavelength increases and the commensurate-to-incommensurate transition also appears simultaneously. In the $(Bi_{2-x}Pb_x)LaCaCuO_{6.5+\delta}$ system, because Pb substitution for Bi does not reduce the length of the b axis markedly, the variation of the modulation vector is not remarkable. Hence, it can be believed that in the Sr-free Bi cuprates, the superstructural modulation is caused by the crystal misfit between the Bi_2O_2 layers and perovskite blocks.

B. Relation of the superstructural modulation and the vibrational properties of oxygen atoms of the Bi_2O_2 layers

In Bi cuprates, due to the existence of superstructural modulation, it can be expected that the distribution of oxygen atoms within the Bi_2O_2 layers is inhomogeneous. Raman-scattering studies[4-6] have revealed that two types of Bi-O bonding exist in the Bi_2O_2 layers. The vibrational frequencies of the oxygen atoms in the two types of Bi-O bonding are about 630 and 660 cm^{-1}. The 660-cm^{-1} mode is generally considered to correspond to vibration of the extra oxygen atoms associated with the superstructural modulation. The work of Qiang *et al.*[12] indicated that this fraction of extra oxygen atoms was inserted between the double BiO layers, while the oxygen atoms corresponding to the $\sim$630-cm^{-1} mode were located in the BiO planes. Yet, from Raman-scattering analyses of the $Bi_2(La_{1-x}Ca_{1+x})CuO_{6.5+\delta}$ system, it can be seen that the vibrational properties of the oxygen atoms in the two types of Bi-O bonding vary with the characteristic of superstructural modulation. With increase in the modulation wavelength, the two kinds of vibrational modes of the oxygen atoms in the Bi_2O_2 layers not only decrease in intensity and linewidth, but also shift to higher frequency. Such a varying behavior of the oxygen-atom vibration can also be explained by the crystal-misfit model. It has already been pointed out that Ca^{2+} substitution for La^{3+} enhances the degree of crystal fit between the BiO layers and perovskite blocks. The structural relaxation caused by this is certain to result in increase in the crystal symmetry, thus weakening the distortion of the Bi_2O_2 layers. Therefore, it can be expected that the linewidth of the Raman peak of the O_{Bi} atoms will decrease gradually with Ca^{2+} substitution for La^{3+}.

This point agrees well with the experimental results. On the other hand, the increase in the vibrational frequency of the O_{Bi} atoms is also likely to be related to the structural relaxation of the layers. But the decrease in the intensity of the 630-cm^{-1} mode caused by Ca^{2+} substitution for La^{3+} possibly originates from decrease in the oxygen content of this system. So, on the whole, we can say that this kind of variation in the vibrational properties of the oxygen atoms in the Bi-O bonding seems to be a consequence of the structural relaxation of the layers. This point of view seems to support the argument of Pham *et al.*[10] that the presence of extra oxygen in the Bi_2O_2 layers can only be regarded as a consequence of the particular geometry introduced by the bismuth, but not as the origin of modulation.

V. CONCLUSIONS

Analyses of the microstructure of the

$Bi_2(La_{1-x}Ca_{1+x})CuO_{6.5+\delta}$

and

$(Bi_{2-x}Pb_x)LaCaCuO_{6.5+\delta}$

systems revealed that these Sr-free Bi cuprates possess a modulation structure similar to that of $Bi_2Sr_2CuO_{6+\delta}$. Moreover, the characteristics of the modulation wave vector depend mainly on the ratio of Ca to La for $Bi_2(La_{1-x}Ca_{1+x})CuO_{6.5+\delta}$ and Bi to Pb for $(Bi_{2-x}Pb_x)LaCaCuO_{6.5+\delta}$. A commensurate-to-incommensurate transition was also observed in the two systems. For the $Bi_2(La_{1-x}Ca_{1+x})CuO_{6.5+\delta}$ system, Raman-scattering analyses showed that a change in the superstructural modulation significantly influenced the vibrational properties of the oxygen atoms of the BiO layers. The intensity and linewidth of the 630-cm^{-1} mode decrease with increase in the modulation wavelength, but the vibrational frequency increased accordingly. The changes in both the modulation vectors and the vibrational properties of the oxygen atoms of the Bi_2O_2 layers are best explained by the crystal-misfit model. The increase in the modulation wavelength comes from enhancement of the degree of crystal fit, and the change of vibrational properties of the oxygen atoms in the Bi-O bonding can be regarded as a consequence of structural relaxation of the layers.

[1]Y. Takemura, M. Hongo, K. Wakaizumi, A. Miyanaga, and S. Yamazaki, Jpn. J. Appl. Phys. **27**, L1864 (1988).
[2]O. Inoue, S. Adachi, Y. Takahashi, H. Hirano, and S. Kawashima, Jpn. J. Appl. Phys. **28**, L778 (1989).
[3]Y. Matsui, A. Maeda, K. Uchinokura, and S. Takekawa, Jpn. J. Appl. Phys. **29**, 273 (1990).
[4]M. Cardona, C. Thomsen, R. Liu, H. G. Von Schnering, M. Hartwey, Y. F. Yan, and Z. X. Zhao, Solid State Commun. **66**, 1225 (1988).
[5]R. Liu, M. V. Klein, P. D. Han, and D. A. Payne, Phys. Rev. B **45**, 7392 (1992).
[6]L. A. Farrow, R. Ramesh, and J. M. Tarascon, Phys. Rev. B **43**, 418 (1991).
[7]H. W. Zandbergen, W. A. Groen, F. C. Mijhoff, G. Tendeloo, and S. Amelinckx, Physica C **156**, 325 (1988).
[8]P. L. Gay and P. Day, Physica C **152**, 335 (1988).
[9]A. K. Cheetham, A. M. Chippendale, and S. J. Hibble, Nature **333**, 21 (1988).
[10]A. Q. Pham, M. Hervieu, A. Maigman, C. Michel, J. Provost, and B. Raveau, Physica C **194**, 243 (1992).
[11]Mao Zhiqiang, Fan Chenggao, Shi Lei, Yao Zhen, Yang Li, Wang Yu, and Zhang Yuheng, Phys. Rev. B **47**, 14 467 (1993).
[12]Q. Wang, R. S. Han, D. L. Yin, and Z. Z. Gan, Phys. Lett. A **168**, 326 (1992).

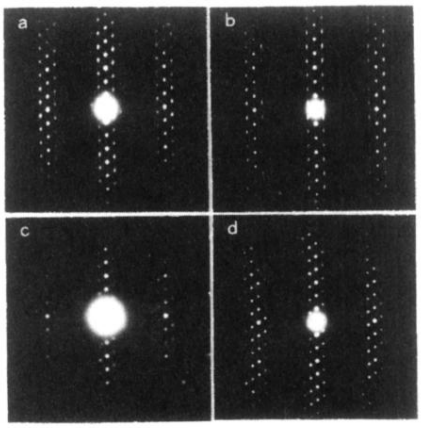

FIG. 2. [100]-zone-axis ED patterns of the samples $Bi_2(La_{1-x}Ca_{1+x})CuO_{6.5+\delta}$; a, $x=0$; b, $x=0.2$; c, $x=0.6$; d, $x=0.8$.

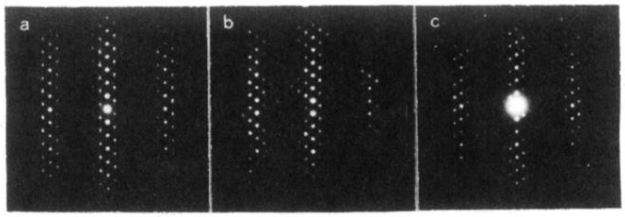

FIG. 3. [100]-zone-axis ED patterns of the samples $(Bi_{2-x}Pb_x)LaCaCuO_{6.5+\delta}$; a, $x=0.1$; b, $x=0.3$; c, $x=0.5$.